applied sciences

MDPI

Article

Adaptive Multi-Dimensional Taylor Network Tracking Control for a Class of Nonlinear Strict Feedback Systems

Qiming Sun [1], Ying Zhang [1,*], Shangzheng Wu [1], Chao Zhang [2] and Xiaochuan Jiang [1]

[1] College of Information Science and Technology, Nanjing Forestry University, Nanjing 210037, China; sqm1122345@126.com (Q.S.); wsz312312@163.com (S.W.); xiaochuanjiang2022@163.com (X.J.)
[2] School of Electrical Engineering and Automation, Henan Institute of Technology, Xinxiang 453003, China; zhangchao915@foxmail.com
* Correspondence: zhangying343@126.com

Abstract: Nonlinear systems are very common in real life, but because they are not superposed and homogeneous, there are many difficulties in controlling nonlinear systems. Therefore, an adaptive control method based on a multi-dimensional Taylor network (MTN) is proposed for a class of nonlinear systems with strict feedback so that the output of the system can track the given signal. In order to achieve the control effect, we define a new state variable and transform the strict feedback system. After transformation, the original feedback system has a standard form, and two parameters to be identified are obtained. Then, the state observer is designed, and the two parameters are identified via the approximation of the MTN. On this basis, the controller design and a system stability analysis are completed. The lemma is introduced, and the stability condition is established by using this low-pass filter to ensure that all closed-loop signals are semi-globally uniform and finally bounded and the output tracking error converges to the residual set near zero. Finally, a numerical simulation of a hydraulic system is carried out to verify the effectiveness of the proposed method. Under the three indexes, the proposed method has obvious advantages.

Keywords: adaptive control; multi-dimensional Taylor network; closed-loop control; strict feedback systems

Citation: Sun, Q.; Zhang, Y.; Wu, S.; Zhang, C.; Jiang, X. Adaptive Multi-Dimensional Taylor Network Tracking Control for a Class of Nonlinear Strict Feedback Systems. *Appl. Sci.* **2023**, *13*, 12864. https://doi.org/10.3390/app132312864

Academic Editor: Tomonobu Senjyu

Received: 24 October 2023
Revised: 17 November 2023
Accepted: 24 November 2023
Published: 30 November 2023

1. Introduction

Non-linear systems are almost ubiquitous in daily life and exist widely in various applications, such as motor [1], power [2], and electrical systems [3]. After more than half a century of development, the control of non-linear systems has made considerable progress, and various control methods and strategies have emerged, e.g., backstepping control strategies [4], neural networks [5], fuzzy-based control [6], and system identification [7].

For example, scenario-based model predictive control (MPC) approaches can mitigate the conservatism inherent in robust open-loop MPC. Reference [8] presents a method for evaluating the confidence intervals of RBNN predictions and determines the number of samples required to estimate the confidence interval for a given confidence level. The authors of [9] propose a security-model-based reinforcement learning approach to control nonlinear systems described by linear parameter variation models.

In order to improve control accuracy, these methods require feedback. For example, a state feedback Smith predictive controller was proposed for the effective temperature control of a cement rotary kiln precalcining furnace [10]. The authors of [11] present a fully distributed adaptive tracking control scheme for multi-agent systems with a strict feedback form. Generally, this type of state feedback control requires all systems' internal state information, which is challenging to achieve in reality.

Therefore, control methods based on system output have also been proposed. These control algorithms require only the system's output information to complete the control process. For example, the authors of [12] studied a linear–quadratic (LQ) control problem with irregular output feedback in which a noisy linear system measured the state. In [13], the authors discuss the collaborative design of output-dependent switching functions and full-order affine filters for discrete-time switched affine systems. This control method has a certain degree of versatility and has achieved good application results. However, the controlled system does not have a strict feedback form.

Strict feedback systems present a good lower triangle form, while the control systems for a flexible manipulator and some temperatures are in a strict feedback form. Commonly, the backstepping control method is used for such systems, e.g., in [14], a neural-network-based adaptive gain scheduling backward sliding mode control (NNAGS-BSMC) method is proposed for a class of non-linear systems with uncertain strict feedback. Reference [15] presents a novel tracking controller utilizing an event-triggering implementation for uncertain rigor feedback systems. Adaptive fuzzy decentralized optimal control problems for a class of large-scale non-linear systems with a strict feedback form have also been studied [16]. A backstepping method usually has specific prerequisite requirements for the system or control strategy and needs to calculate a higher differential, imposing a high calculation complexity. Such problems have been improved to a certain extent by combining some improved backstepping methods with adaptive control ideas. For example, [17] addresses the adaptive event-triggered control of non-linear continuous-time strict feedback systems. However, the overall calculation process of this method must meet trigger conditions before it is carried out, prohibiting it from meeting real-time performance requirements.

With the development of neural networks, new methods have been proposed for non-linear control problems, exploiting the appealing approximation characteristics of neural networks. For example, [18] addresses the compound learning control of a perturbed uncertain strict feedback system. In [19], the authors studied the data-based compound neural control of an uncertain strict feedback system's online record using a backstepping framework. This algorithm provides a relatively general idea for non-linear control to a certain extent, but as neuron cardinality increases, the computational complexity increases geometrically. The multi-dimensional Taylor network is a newly proposed control structure. Due to its simple structure and convenient application, some promising results have been achieved. For example, the authors of [20] studied non-linear time-delay systems with uncertainties. However, the use of the MTN control algorithm for a strict feedback system has not been thoroughly studied.

Spurred by this, this paper proposes an output feedback control method for a strict non-linear system based on an MTN so that the system's output can automatically track the desired signal. Our method initially transforms the original non-linear strict feedback system and redefines the state variables to obtain the new standard form. The state observer then completes the identification process of the adaptive system with the MTN's good approximation characteristics. The adaptive control law completes the system's tracking output based on this. Finally, a numerical simulation of a servo-hydraulic system model is carried out, verifying the effectiveness of the proposed algorithm.

The main contributions of this paper are as follows:

1. The traditional MTN control method relies on the unique performance of its basic structure and is designed and used for general controlled objects. Therefore, some characteristics of the controlled object itself are not fully considered and utilized. Therefore, this paper applies the MTN to strictly nonlinear feedback systems for the first time, taking full advantage of the characteristics that different parameters of the MTN can have different outputs with the same result and that processing two sets of internal parameters at the same time can effectively improve control efficiency.
2. In the control process, a set of variable representation rules is designed so that the general strict feedback system can be expressed in a standard form. On this basis, an adaptive parameter-adjustment rule based on a state observer is designed to bring the tracking error close to 0. Thanks to the simple structure of the MTN, compared with a neural network algorithm, it can effectively reduce the number of calculations.

The remainder of this paper is organized as follows. Section 2 introduces the strict feedback system and transforms the original system into a standard form. Section 3 presents the design of the state observer, while Section 4 introduces the multi-dimensional Taylor network and its basic structure. Section 5 introduces a parameter identification method based on a multi-dimensional Taylor network, and Section 6 presents the controller's design and a stability analysis of the system. Section 7 illustrates the effectiveness of the proposed control scheme through a numerical simulation of a hydraulic control system. Finally, Section 8 concludes this paper.

2. System Model

Consider the following strictly non-linear feedback system:

$$\begin{cases} \dot{x}_1 = f_1(x_1) + h_1(x_1)x_2 \\ \vdots \\ \dot{x}_i = f_i(\boldsymbol{x}_i) + h_i(\boldsymbol{x}_i)x_{i+1} \\ \vdots \\ \dot{x}_n = f_n(\boldsymbol{x}_n) + h_n(\boldsymbol{x}_n)u \\ y = x_1 \end{cases} \tag{1}$$

where $\boldsymbol{x}_i = [x_1, x_2, \cdots, x_i] \in R^i$, $i = 1, 2, \cdots, n$ is the system state variable, $u \in R$ is the system control input, $y \in R$ is the system output, $f_i(\cdot)$, $i = 1, 2, \cdots, n$ is the non-linear system mapping, $h_i(\cdot)$, $i = 1, 2, \cdots, n$ is the system's non-linear control gain function, and $h_i(\cdot), \ldots, h_i(\cdot)$ are not equal to 0.

The main task of this paper is designing an MTN-based output feedback controller for the above-mentioned strictly non-linear feedback system, affording the output of the system y to track a given signal y_d.

Traditional control methods usually require all state variable information for such problems, that is, $x_1, x_2, \cdots, x_n$. At the same time, the multi-step backstepping controller design suffers from error accumulation, and the process is complicated and cumbersome. Thus, this paper proposes a feedback algorithm based only on the output to simplify the control algorithm and reduce the calculation burden. In order to realize the control algorithm, the original strict feedback system needs to be transformed.

We define the state variables as

$$\begin{cases} z_1 = x_1 \\ \vdots \\ z_i = \dot{z}_{i-1} \quad i = 2, \cdots, n \\ y = x_1 = z_1 \end{cases} \tag{2}$$

Then, there is

$$z_2 = \dot{z}_1 = \dot{x}_1 \tag{3}$$

$$\begin{aligned} z_3 = \dot{z}_2 &= \tfrac{\partial f_1}{\partial x_1}\dot{x}_1 + \tfrac{\partial h_1}{\partial x_1}\dot{x}_1 x_2 + h_1 \dot{x}_2 \\ &= \tfrac{\partial f_1}{\partial x_1}\dot{x}_1 + \tfrac{\partial h_1}{\partial x_1}\dot{x}_1 x_2 + h_1(f_2 + h_2 x_3) \\ &= (\tfrac{\partial f_1}{\partial x_1} + \tfrac{\partial h_1}{\partial x_1}x_2)(f_1 + h_1 x_2) + h_1 f_2 + h_1 h_2 x_3 \end{aligned} \tag{4}$$

Setting $A_2 = (\frac{\partial f_1}{\partial x_1} + \frac{\partial h_1}{\partial x_1}x_2)(f_1 + h_1 x_2) + h_1 f_2$ and $B_2 = h_1 h_2$, we obtain

$$z_3 = \dot{z}_2 = A_2 + B_2 x_3 \tag{5}$$

By analogy, Equation (5) can be expressed as

$$\dot{z}_i = A_i + B_i x_{i+1} \tag{6}$$

where $A_i = \sum_{k=1}^{i-1}(\frac{\partial A_{i-1}}{\partial x_k} + \frac{\partial B_{i-1}}{\partial x_k}x_i)(f_k + h_k x_{k+1}) + B_{i-1}f_i$ and $B_i = B_{i-1}h_i = B_{i-2}h_{i-1}h_i = \prod_{k=1}^{i} h_k$.

After the above changes, the original strict-feedback non-linear system can be expressed as

$$\begin{cases} \dot{z}_1 = z_2 \\ \dot{z}_2 = z_3 \\ \vdots \\ \dot{z}_{i-1} = z_i i = 2, \cdots, n-1 \\ \vdots \\ \dot{z}_n = A_n + B_n u \\ y = z_1 \end{cases} \quad (7)$$

In addition, A_n and B_n include the unknown non-linear mappings f_i and h_i of the original system. Since h_i in the original hypothesis is not equal to 0, it is assumed that the gain function B_n is a bounded function greater than 0 and that $0 < B_{\min} \le B_n \le B_{\max}$, where $B_{\min}$ and $B_{\max}$ are constants greater than 0.

After the transformation, the original strict feedback system has a general standard shape. Since $z_1 = x_1$, after the transformation, the system output is unchanged, and the original control target is consistent. However, A_n and B_n are unknown, and except for z_1, the higher-order state z_i is unavailable, so a state observer needs to be designed.

3. State Observer

According to [21], for the above-mentioned strict feedback system, the following state observer can be constructed to observe the high-order state of z.

$$\begin{cases} \dot{\hat{z}}_1 = \alpha_1 \\ \alpha_1 = K_1|y - \hat{z}_1|^{\frac{n}{n+1}} sign(y - \hat{z}_1) + \hat{z}_2 \\ \vdots \\ \dot{\hat{z}}_i = \alpha_i \\ \alpha_i = K_i|\alpha_{i-1} - \hat{z}_i|^{\frac{n-i+1}{n-i+2}} sign(\alpha_{i-1} - \hat{z}_i) + \hat{z}_{i+1} \quad i = 2, \cdots, n-1 \\ \vdots \\ \dot{\hat{z}}_n = \alpha_n \\ \alpha_n = K_n|\alpha_{n-1} - \hat{z}_n|^{\frac{1}{2}} sign(\alpha_{n-1} - \hat{z}_n) + \hat{z}_{n+1} \\ \dot{\hat{z}}_{n+1} = K_{n+1} sign(\alpha_n - \hat{z}_{n+1}) \end{cases} \quad (8)$$

where $K_1, \cdots, K_{n+1} > 0$ is the observation gain and $\hat{z}_1, \cdots, \hat{z}_n$ is the estimation of the state quantity $z_1, \cdots, z_n$. It has been proven in the literature that the above observer converges in a finite time.

4. Experimental Investigation

The MTN can approximate any non-linear functions with a finite point of discontinuity. A neat structure is the merit of the MTN, whose terms are easy to adjust. For further details on the MTN, the reader is referred to [22–28].

Let

$$\mathbf{z} = [z_1, z_2, \ldots z_n] \quad (9)$$

The basic structure of the MTN is illustrated in Figure 1.

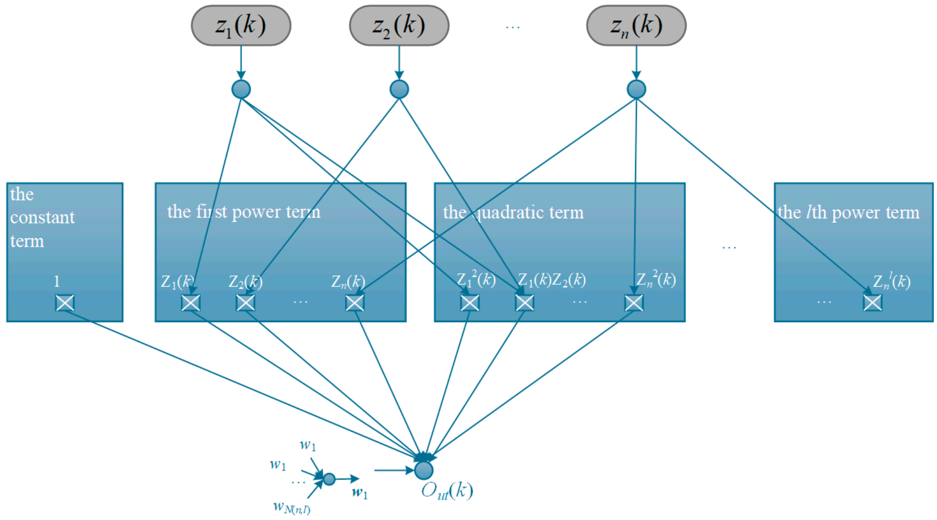

Figure 1. Basic structure of MTN.

In other words, there exists a set of parameter vectors $\boldsymbol{w} = [w_1, w_2, \ldots w_{N(n,t)}]$ such that the output of the MTN O_{ut} can be expressed as

$$O_{ut} = \sum_{i=1}^{N(n,t)} w_i \prod_{s=1}^{n} z_i^{\lambda_{s,i}} \tag{10}$$

where $N(n,t)$ is the total number of the expansion, w_i is the weight of the product term, $\lambda_{s,i}$ is the power of z_s in the ith product term, and $\sum_{s=1}^{n} \lambda_{s,i} \leq t$.

Setting $\eta(\mathbf{z}) = [1, z_1, z_2, \ldots, z_n, \ldots, z_1^2, z_1 z_2, \ldots, z_n^t]^T$, we obtain

$$O_{ut} = \boldsymbol{w} \cdot \eta(\mathbf{z}) \tag{11}$$

Similar to Reference [29], there is no fixed standard for the highest power of the MTN, but with an increase in the power of the MTN, the internal function will increase, and it is usually appropriate to choose three times in practice.

5. Adaptive System Identification

In order to design an ideal feedback controller, A_n and B_n are required; thus, system identification is involved, with traditional identification methods usually considering A_n and B_n separately. Due to problems in B_n such as zero crossing, it is easy to cause singularity problems like system divergence. To solve this difficulty, we modify the system as follows.

We rewrite the last subsystem and obtain

$$u = \frac{1}{B_n} \dot{z}_n - \frac{A_n}{B_n} \tag{12}$$

Therefore, the system can be identified for the two unknowns $\frac{1}{B_n}$ and $\frac{A_n}{B_n}$ to avoid the singularity problem.

According to the basic structure of MTN, we obtain

$$\begin{cases} \frac{1}{B_n} = \boldsymbol{w}_1^{*\mathrm{T}} \eta(\mathbf{z}) + \varepsilon_1 \\ \frac{A_n}{B_n} = \boldsymbol{w}_2^{*\mathrm{T}} \eta(\mathbf{z}) + \varepsilon_2 \end{cases} \tag{13}$$

where $\eta(\mathbf{z})$ is the polynomial combination of MTN.

Since $\mathbf{z}$ is unknown, it can be replaced by $\hat{\mathbf{z}}$ from the foregoing equation. Despite an error between them, it can be compensated through weight adjustment. $\boldsymbol{w}_1^*$ and $\boldsymbol{w}_2^*$ are ideal-weight MTN vectors.

Unlike traditional neural network methods, our technique requires two sets of basis vectors in which each is calculated separately, imposing a significant computational burden. Moreover, there is a suitable polynomial combination compared with the MTN, i.e., the identification effect can be achieved only by changing the parameter value.

By introducing the MTN, the system input value can be rewritten as

$$u = \boldsymbol{w}_1^{*\mathrm{T}} \eta(\mathbf{z}) \dot{z}_n - \boldsymbol{w}_2^{*\mathrm{T}} \eta(\mathbf{z}) + \varepsilon \tag{14}$$

where $\varepsilon = \varepsilon_1 \dot{z}_n - \varepsilon_2$ is the total error of the MTN.

In the above formula, $\dot{z}_n$ is unknown and can be replaced by $\dot{\hat{z}}_n$, so we can obtain

$$u = \boldsymbol{w}_1^{*\mathrm{T}} \eta(\hat{\mathbf{z}}) \dot{\hat{z}}_n - \boldsymbol{w}_2^{*\mathrm{T}} \eta(\hat{\mathbf{z}}) + \xi \tag{15}$$

where $\xi = \varepsilon + \boldsymbol{w}_1^{*\mathrm{T}} \eta(\hat{\mathbf{z}}) \dot{\tilde{z}}_n$ is the total system identification error.

Since the unknown network weights $\boldsymbol{w}_1^*$ and $\boldsymbol{w}_2^*$ have not been estimated, the control strategy described below is designed.

In the above calculations, only $\hat{z}_n$ is estimated, while the derivative of the system $\hat{z}_n$, i.e., $\dot{\hat{z}}_n$, is unknown. Thus, a low-pass filter $\frac{1}{1+\theta s}$ is introduced where θ is the filter constant. Using the inverse Laplace transform and without considering the influence of the initial value, the following formula can be obtained:

$$\begin{cases} \hat{z}_{n\theta} = \frac{\hat{z}_n}{1+\theta s} \\ \dot{\hat{z}}_{n\theta} = \frac{\hat{z}_n - \hat{z}_{n\theta}}{\theta} \end{cases} \tag{16}$$

letting the initial value of $\hat{z}_{n\theta}$ be 0, i.e., $\hat{z}_{n\theta}(0) = 0$.

Correspondingly, the low-pass filter can be applied to other variables, and the initial value is set to 0.

Lemma 1. *Consider the continuous function $G(x) = G_1(x)G_2(x)$, where $G_1(x)$ and $G_2(x)$ are both continuous mappings. After applying the low-pass filter, the following conclusions can be drawn:*

$$G_\theta(x) = G_{1\theta}(x) G_{2\theta}(x) + \rho \tag{17}$$

where $G_{1\theta}$ and $G_{2\theta}$ are the functions of G_1 and G_2 passing through the low-pass filter and ρ is the high-order truncation error.

From Lemma 1, we obtain

$$(\eta(\hat{\mathbf{z}}) \dot{\hat{z}}_n)_\theta = \eta(\hat{\mathbf{z}})_\theta \dot{\hat{z}}_{n\theta} + \rho \tag{18}$$

Substituting the previous formula, we obtain

$$u_\theta = \boldsymbol{W}^{*\mathrm{T}} \Psi_\theta + \lambda \tag{19}$$

where $\lambda = \rho + \xi_\theta$ is the lumped error, $\boldsymbol{W}^* = [\boldsymbol{w}_1^{*\mathrm{T}}, \boldsymbol{w}_2^{*\mathrm{T}}]^{\mathrm{T}}$ is the generalized weight vector, and $\Psi_\theta = [\frac{\eta(\hat{\mathbf{z}})_\theta (\hat{z}_n - \hat{z}_{n\theta})}{\theta}, -\eta(\hat{\mathbf{z}})_\theta]$ is the generalized control vector of input u.

6. Adaptive Control Law Design

By adjusting $\hat{\boldsymbol{W}}$ to make it infinitely close to $\boldsymbol{W}^*$, we finally achieve the control purpose. To this end, we designed an error-based adaptive adjustment rate that is $\widetilde{\boldsymbol{W}} = \boldsymbol{W}^* - \hat{\boldsymbol{W}}$.

Parameter definition:

$$F = \frac{\beta \Psi_\theta}{\Psi_\theta^{\mathrm{T}} \Psi_\theta + \gamma} \tag{20}$$

where β and γ are positive constants.

We design two auxiliary variables, $P \in R^{2N \times 2N}$ and $Q \in R^{2N \times 1}$, based on F:

$$\begin{cases} \dot{P} = -\beta P + F\Psi_\theta^{\mathrm{T}} & P(0) = 0 \\ \dot{Q} = -\beta Q + F u_\theta^{\mathrm{T}} & Q(0) = 0 \end{cases} \tag{21}$$

Since both β and γ are greater than 0, it can be guaranteed that P and Q are both bounded.

We calculate the above formula to obtain

$$Q = P\boldsymbol{W}^* - \int_0^t e^{\beta(\tau - t)} F \lambda d\tau \tag{22}$$

By setting $\delta = \int_0^t e^{\beta(\tau - t)} F \lambda d\tau$, we obtain

$$Q = P\boldsymbol{W}^* - \delta \tag{23}$$

where the norm of δ is a bounded function, that is, $\|\delta\| \le \delta_{\max}$.

The error vector is defined as

$$S = P\hat{\boldsymbol{W}} - Q \tag{24}$$

By subtracting the above two formulas, we obtain

$$S = \delta - P\widetilde{\boldsymbol{W}} \tag{25}$$

Then, after the low-pass filter, the auxiliary variables F, P, and Q are calculated and S is obtained. An adaptive rate based on S can be designed as

$$\Delta \hat{\boldsymbol{W}} = -\lambda \cdot S \tag{26}$$

where $\lambda > 0$ is an adaptive adjustment step.

Theorem 1. *If the above-mentioned adaptive rate is used, the weight error vector finally converges near the 0 point under the condition of a continuous excitation of Ψ_θ.*

Proof. We define the Lyapunov function as

$$V = \frac{1}{2} \widetilde{\boldsymbol{W}}^{\mathrm{T}} Step^{-1} \widetilde{\boldsymbol{W}} \tag{27}$$

Deriving the above formula provides

$$\dot{V} = \widetilde{\boldsymbol{W}}^{\mathrm{T}} Step^{-1} \dot{\widetilde{\boldsymbol{W}}} = \widetilde{\boldsymbol{W}}^{\mathrm{T}} \delta - \widetilde{\boldsymbol{W}}^{\mathrm{T}} P \widetilde{\boldsymbol{W}} \tag{28}$$

Since Ψ_θ continues to excitate, there is a normal number, κ, for $\forall t > 0$:

$$\int_t^{t+\Delta t} F \Psi_\theta^{\mathrm{T}} d\tau \ge \kappa I \tag{29}$$

It can be seen from the auxiliary variable P that

$$P(t) \ge e^{-\beta \Delta t} \int_{t-\Delta t}^{t} F \Psi_\theta^{\mathrm{T}} d\tau \ge e^{-\beta \Delta t} \kappa \tag{30}$$

For simplicity, we define $\varsigma = e^{-\beta\Delta t}\kappa$ and obtain

$$\dot{V} = \widetilde{\boldsymbol{W}}^{\mathrm{T}}\delta - \widetilde{\boldsymbol{W}}^{\mathrm{T}}P\widetilde{\boldsymbol{W}} \leq \frac{\delta_{\max}^2}{2\varsigma} - \frac{\varsigma}{\lambda_{\max}(Step^{-1})}V \tag{31}$$

Since both $\frac{\delta_{\max}^2}{2\varsigma}$ and $\frac{\varsigma}{\lambda_{\max}(Step^{-1})}$ are greater than 0, it can be known from the Lyapunov theorem that V and the error vector $\widetilde{\boldsymbol{W}}$ converge to around 0 according to the exponential law.

The proof is complete. □

Compared with the traditional gradient method, the auxiliary variables F, P, and Q are constructed in this paper, and then an adaptive rate based on S is designed, ensuring that the error vector $\widetilde{\boldsymbol{W}}$ converges to near 0, i.e., $\hat{\boldsymbol{W}}$ is infinitely close to $\boldsymbol{W}^*$. Thus, the system estimation affords guaranteed accuracy.

Controller Design and Stability Analysis

In order to achieve the ultimate control goal, we define the error vector and the generalized Hurwitz polynomial

$$\boldsymbol{e} = \mathbf{z} - \boldsymbol{x_d} \tag{32}$$

where $\boldsymbol{x_d} = [x_d, \cdots, x_d^{(n-1)}]$ are the tracking target and its higher-order derivative.

Set

$$\nu = [\boldsymbol{\Lambda}^{\mathrm{T}}, 1]\boldsymbol{e} \tag{33}$$

where $\boldsymbol{\Lambda} = [\Lambda_1, \cdots, \Lambda_{n-1}]^{\mathrm{T}}$ makes $\Lambda_1 + \Lambda_2 s + \cdots + \Lambda_{n-1}s^{n-2} + s^{n-1}$ satisfy the Hurwitz polynomial.

When ν converges and is bounded, $\boldsymbol{e}$ also converges and is bounded accordingly.

Here, the observation state $\hat{\mathbf{z}}$ is used instead of $\mathbf{z}$, and the actual errors $\hat{\boldsymbol{e}}$ and $\hat{\nu}$ are defined accordingly. That is,

$$\hat{\boldsymbol{e}} = \hat{\mathbf{z}} - \boldsymbol{x_d} \tag{34}$$

$$\hat{\nu} = [\boldsymbol{\Lambda}^{\mathrm{T}}, 1]\hat{\boldsymbol{e}} \tag{35}$$

The difference between the replacement and the original state is represented by $\widetilde{\mathbf{z}}$ and $\widetilde{\nu}$, as shown below.

$$\widetilde{\mathbf{z}} = \boldsymbol{e} - \hat{\boldsymbol{e}} = (\mathbf{z} - \boldsymbol{x_d}) - (\hat{\mathbf{z}} - \boldsymbol{x_d}) = \mathbf{z} - \hat{\mathbf{z}} \tag{36}$$

$$\widetilde{\nu} = \nu - \hat{\nu} = [\boldsymbol{\Lambda}^{\mathrm{T}}, 1]\widetilde{\mathbf{z}} \tag{37}$$

Taking the derivative of ν, we obtain

$$\dot{\nu} = [0, \boldsymbol{\Lambda}^{\mathrm{T}}]\boldsymbol{e} + A_n + B_n u - x_d^{(n)} \tag{38}$$

We multiply both ends of the equation by $\frac{1}{B_n}$, substitute the expressions above, and sort them to obtain

$$\frac{1}{B_n}\dot{\nu} = \boldsymbol{w}_1^{*\mathrm{T}}\eta(\mathbf{z})[0, \boldsymbol{\Lambda}^{\mathrm{T}}]e + \varepsilon_1[0, \boldsymbol{\Lambda}^{\mathrm{T}}]\boldsymbol{e} + \boldsymbol{w}_2^{*\mathrm{T}}\eta(\mathbf{z}) + \varepsilon_2 + u - \boldsymbol{w}_1^{*\mathrm{T}}\eta(\mathbf{z})x_d^{(n)} - \varepsilon_1 x_d^{(n)} \tag{39}$$

We replace $\mathbf{z}$ with the observation state $\hat{\mathbf{z}}$. Let $\Phi = [\eta(\hat{\mathbf{z}})[0, \boldsymbol{\Lambda}^{\mathrm{T}}]\hat{e} - \eta(\hat{\mathbf{z}})x_d^{(n)}, \eta(\hat{\mathbf{z}})]$ be the augmented polynomial vector, and let $\rho = (\boldsymbol{w}_1^{*\mathrm{T}}\eta(\hat{\mathbf{z}}) + \varepsilon_1)[0, \boldsymbol{\Lambda}^{\mathrm{T}}]\widetilde{\mathbf{z}} + \varepsilon_2 - \varepsilon_1 x_d^{(n)}$ be the sum of the approximation errors of the differential observer and the MTN network. Then, we obtain

$$\frac{1}{B_n}\dot{\nu} = \boldsymbol{W}^{*\mathrm{T}}\Phi + \varepsilon_1[0, \boldsymbol{\Lambda}^{\mathrm{T}}]\hat{\boldsymbol{e}} + \rho + u \tag{40}$$

In order to achieve the final control purpose, the control quantity u is constructed as shown below.

$$u = -k\hat{v} - \hat{\boldsymbol{w}}_1^{\mathrm{T}}\eta(\hat{\mathbf{z}})[0, \boldsymbol{\Lambda}^{\mathrm{T}}]\hat{\boldsymbol{e}} - x_d^{(n)} - \hat{\boldsymbol{w}}_2^{\mathrm{T}}\eta(\hat{\mathbf{z}}) \tag{41}$$

Where k is the gain parameter, and $\hat{\boldsymbol{w}}_1$ and $\hat{\boldsymbol{w}}_2$ are estimates of the ideal weight vectors $\hat{\boldsymbol{w}}_1^*$ and $\hat{\boldsymbol{w}}_2^*$.

We substitute u to obtain

$$\frac{1}{B_n}\dot{v} = -k\hat{v} + \widetilde{\boldsymbol{W}}^{\mathrm{T}}\Phi + \rho + \varepsilon_1[0, \boldsymbol{\Lambda}^{\mathrm{T}}]\hat{\boldsymbol{e}} \tag{42}$$

Similar to Theorem 1, the following adaptive law is designed:

$$\Delta\hat{\boldsymbol{W}} = -Step \cdot (\beta S - \Phi\hat{v}) \tag{43}$$

where $Step > 0$ is the adaptive adjustment step and $\beta > 0$ is the correction parameter.

Theorem 2. *Given the strict feedback system of Equation (1), when the differential state observer of Equation (8), the control input of Equation (41), the parameter vector adaptive law of Equation (43), and the MTN polynomial $\eta(\mathbf{z})$ preserve a continuous motivation, then all signals in a closed-loop system are bounded and the error variables $\boldsymbol{e}$ and ν and the weight vector error $\widetilde{\boldsymbol{W}}$ all converge to a compact set near the 0 point.*

Proof. From the definition of the observation error, we obtain

$$\frac{1}{B_n}\dot{\hat{v}} = -k\hat{v} + \widetilde{\boldsymbol{W}}^{\mathrm{T}}\Phi + \rho + \varepsilon_1[0, \boldsymbol{\Lambda}^{\mathrm{T}}]\hat{\boldsymbol{e}} + \frac{1}{B_n}[\boldsymbol{\Lambda}^{\mathrm{T}}, 1]\widetilde{\mathbf{z}} \tag{44}$$

Let $\gamma = \rho + \frac{1}{B_n}[\boldsymbol{\Lambda}^{\mathrm{T}}, 1]\widetilde{\mathbf{z}}$ be the observation error of the differentiator and bounded, that is, $\gamma \leq \gamma_{\max}$, where $\gamma_{\max}$ is a normal constant.

We choose the Lyapunov function as follows:

$$V = \frac{1}{2}\hat{v}^2 + \frac{1}{2}B_{\min}\widetilde{\boldsymbol{W}}^{\mathrm{T}}Step^{-1}\widetilde{\boldsymbol{W}} \tag{45}$$

By deriving the above formula, we obtain

$$\dot{V} = \hat{v}\dot{\hat{v}} + B_{\min}\widetilde{\boldsymbol{W}}^{\mathrm{T}}Step^{-1}\dot{\widetilde{\boldsymbol{W}}} \tag{46}$$

Substituting the previous form into Equation (41), we obtain

$$\begin{aligned}\dot{V} = &-B_n k\hat{v}^2 + (B_n - B_{\min})\widetilde{\boldsymbol{W}}^{\mathrm{T}}\Phi\hat{v} + B_n\varepsilon_1[0, \boldsymbol{\Lambda}^{\mathrm{T}}]\hat{\boldsymbol{e}}\hat{v} \\ &+B_n\gamma\hat{v} - B_{\min}\beta\widetilde{\boldsymbol{W}}^{\mathrm{T}}P\widetilde{\boldsymbol{W}} + B_{\min}\beta\widetilde{\boldsymbol{W}}^{\mathrm{T}}\delta\end{aligned} \tag{47}$$

From Equation (35), we know that $|\hat{v}| \geq \frac{|\hat{e}|}{\lambda_{\min}([\boldsymbol{\Lambda}^{\mathrm{T}},1])}$, so we obtain

$$\begin{aligned}\dot{V} \leq &-B_n k\hat{v}^2 + (B_n - B_{\min})\widetilde{\boldsymbol{W}}^{\mathrm{T}}\Phi\hat{v} + B_n\gamma\hat{v} + B_n\varepsilon_1\tfrac{\lambda_{\max}([0,\boldsymbol{\Lambda}^{\mathrm{T}}])}{\lambda_{\min}([\boldsymbol{\Lambda}^{\mathrm{T}},1])}|\hat{v}|^2 \\ &-B_{\min}\beta\widetilde{\boldsymbol{W}}^{\mathrm{T}}P\widetilde{\boldsymbol{W}} + B_{\min}\beta\widetilde{\boldsymbol{W}}^{\mathrm{T}}\delta \\ \leq &-B_n(k - \varepsilon_1\tfrac{\lambda_{\max}([0,\boldsymbol{\Lambda}^{\mathrm{T}}])}{\lambda_{\min}([\boldsymbol{\Lambda}^{\mathrm{T}},1])})\hat{v}^2 + (B_n - B_{\min})\widetilde{\boldsymbol{W}}^{\mathrm{T}}\Phi\hat{v} \\ &+B_n\gamma\hat{v} - B_{\min}\beta\widetilde{\boldsymbol{W}}^{\mathrm{T}}P\widetilde{\boldsymbol{W}} + B_{\min}\beta\widetilde{\boldsymbol{W}}^{\mathrm{T}}\delta\end{aligned} \tag{48}$$

Therefore, $k - \varepsilon_1\frac{\lambda_{\max}([0,\boldsymbol{\Lambda}^{\mathrm{T}}])}{\lambda_{\min}([\boldsymbol{\Lambda}^{\mathrm{T}},1])} > 0$ can be established by setting a larger k.

From Theorem 1, we know that $\lambda_{\min}(P) > \kappa$, so we have

$$\begin{aligned}\dot{V} \le & -B_n\left(k - \varepsilon_1 \frac{\lambda_{\max}([0,\mathbf{\Lambda}^{\mathrm{T}}])}{\lambda_{\min}([\mathbf{\Lambda}^{\mathrm{T}},1])}\right)\hat{v}^2 + (B_{\max} + B_{\min})\left\|\widetilde{\boldsymbol{W}}^{\mathrm{T}}\Phi\right\||\hat{v}| \\ & + B_n\gamma_{\max}|\hat{v}| - B_{\min}\beta\kappa\left\|\widetilde{\boldsymbol{W}}\right\|^2 + B_{\min}\beta\left\|\widetilde{\boldsymbol{W}}\right\|\delta_{\max}\end{aligned} \tag{49}$$

By applying Young's inequality to $\left\|\widetilde{\boldsymbol{W}}^{\mathrm{T}}\Phi\right\||\hat{v}|$, $B_n\gamma_{\max}|\hat{v}|$, and $\left\|\widetilde{\boldsymbol{W}}\right\|\delta_{\max}$, and substituting the result into the above formula, we obtain

$$\begin{aligned}\dot{V} \le & -\min\left\{B_n\left(k - \varepsilon_1 \frac{\lambda_{\max}([0,\mathbf{\Lambda}^{\mathrm{T}}])}{\lambda_{\min}([\mathbf{\Lambda}^{\mathrm{T}},1])}\right) - \frac{2(B_{\max}+B_{\min})\|\Phi\|^2}{\kappa B_{\min}\beta}, \frac{\beta\kappa}{\lambda_{\max}([0,\mathbf{\Lambda}^{\mathrm{T}}])}\right\}V \\ & + \frac{B_{\max}^2\gamma_{\max}^2}{2B_{\min}\left(k - \varepsilon_1 \frac{\lambda_{\max}([0,\mathbf{\Lambda}^{\mathrm{T}}])}{\lambda_{\min}([\mathbf{\Lambda}^{\mathrm{T}},1])}\right)} + \frac{B_{\min}\beta\delta_{\max}^2}{\kappa}\end{aligned} \tag{50}$$

Equation (50) reveals that by appropriately increasing the gain parameter k and the correction parameter β, it can be ensured that

$$\min\left\{B_n\left(k - \varepsilon_1 \frac{\lambda_{\max}([0,\mathbf{\Lambda}^{\mathrm{T}}])}{\lambda_{\min}([\mathbf{\Lambda}^{\mathrm{T}},1])}\right) - \frac{2(B_{\max}+B_{\min})\|\Phi\|^2}{\kappa B_{\min}\beta}, \frac{\beta\kappa}{\lambda_{\max}([0,\mathbf{\Lambda}^{\mathrm{T}}])}\right\} > 0 \tag{51}$$

$$\frac{B_{\max}^2\gamma_{\max}^2}{2B_{\min}\left(k - \varepsilon_1 \frac{\lambda_{\max}([0,\mathbf{\Lambda}^{\mathrm{T}}])}{\lambda_{\min}([\mathbf{\Lambda}^{\mathrm{T}},1])}\right)} + \frac{B_{\min}\beta\delta_{\max}^2}{\kappa} > 0 \tag{52}$$

From the Lyapunov theorem, we know that the errors $\hat{v}$ and $\widetilde{\boldsymbol{W}}$ are bounded and converge to a compact set near the 0 point. At the same time, from Equations (35) and (43), and since $\widetilde{\mathbf{z}}$ is bounded, we conclude that ν, $\boldsymbol{e}$, and $\hat{\boldsymbol{e}}$ are bounded and that the weight vector $\hat{\boldsymbol{W}}$ is bounded. From Equation (41), the control signal u is bounded.

The proof is completed. □

In this paper, the adaptive law based on an MTN ensures that the estimated weight vector approaches the true weight vector in a direction with infinitely small errors. At the same time, compared with the traditional dual-neural-network identification method, the number of calculations is reduced, and the identification process of the unknown dynamics of the entire system is completed.

7. Simulation Example

Consider the servo-hydraulic system of [28], as illustrated in Figure 2.

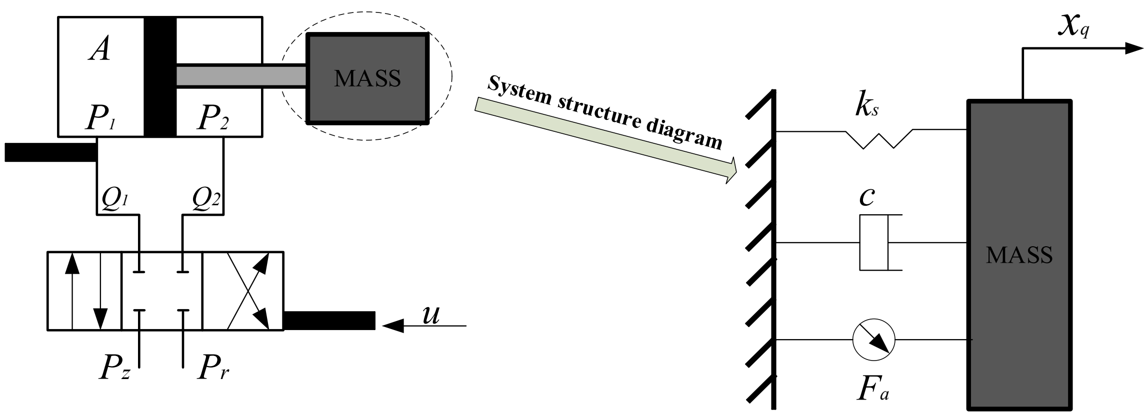

Figure 2. Schematic diagram of servo-hydraulic system.

The system has typical strict-feedback non-linear characteristics where x_q is the output displacement, F_a is the output driving force of the hydraulic drive, P_i is the pressure, m is the mass of the load, k_s is the spring coefficient, and c is the damping coefficient.

The system model is as follows:

$$\begin{cases} \dot{x}_1 = x_2 \\ \dot{x}_2 = -f_{11}(x)x_1 - f_{12}(x)x_2 + x_3 \\ \dot{x}_3 = -f_{21}(x)x_2 - f_{22}(x)x_3 + f_{23}(x)u \\ y = x_1 \end{cases} \tag{53}$$

where $f_{11}(x) = \frac{k_s}{m}$, $f_{12}(x) = \frac{c}{m}$, $f_{21}(x) = \frac{4\beta_e\omega^2}{V_t m}$, $f_{22}(x) = \frac{4\beta_e}{V_t m}C_t$, and $f_{23}(x) = \frac{4\beta_e\omega}{V_t m}\chi$.

V_t is the total volume of the hydraulic cylinder, β_e is the elastic modulus of the hydraulic fluid, ω is the effective acting area of the piston in the hydraulic cylinder, and χ is the effective conversion ratio of the servo valve input and output.

In order to verify the validity, we select data close to reality:

$m = 38$ kg; $k_s = 1.425 \times 10^4$ N/m; $c = 1.425 \times 10^3$ N $\cdot$ s/m; $V_t = 5.6 \times 10^{-5}$ m^3; $\beta_e = 600$ MP$_a$; $\omega = 2.8 \times 10^{-4}$ m^2; $C_t = 4 \times 10^{-13}$ m$^3 \cdot$ P$_a$/s; $\chi = 1 \times 10^{-2}$ m$^3 \cdot$ V/s.

The unit step response curve of the MTN is illustrated in Figure 3.

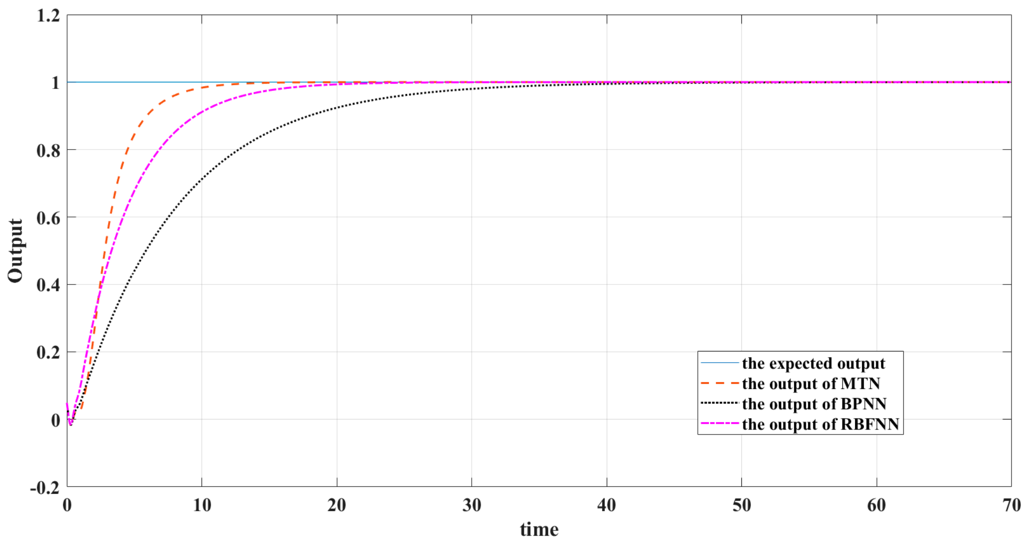

Figure 3. Output comparison.

In Figure 3, the BPNN controller and RBFNN controller are given. As traditional control methods, the neural network controllers work well and have the ability to resist disturbance. From these experimental results, it is shown that the method proposed in this paper is faster than another.

To accurately assess the performance of the three control methods, we employed three error metrics: the (1) Root Mean Square Error (RMSE), which represents the square root of the ratio of the squared differences between the actual values and the predicted values and is sensitive to outliers in the data; (2) the Mean Absolute Error (MAE), which measures the average distance between the model's predicted values and the actual values and is less sensitive to outliers; and (3) the Mean Absolute Percentage Error (MAPE), which is a relative measure that quantifies the accuracy of predictions using relative error. The values of these metrics obtained using the three control methods are shown in Table 1.

Table 1. The unit step response comparison among three metrics obtained using different control methods.

Error Comparison	RMSE	MAE	MAPE
MTN	0.03360	0.04857	1.0844
BPNN controller	0.06321	0.11697	1.18105
RBF controller	0.03682	0.06465	1.15638

As shown in Table 1, the proposed method outperforms the NN and the RBF in terms of most metrics.

In order to verify the tracking performance of the system, $y_d = 1 + 0.1\sin(t)$ was chosen as the desired signal, and the system outputs are illustrated in Figure 4.

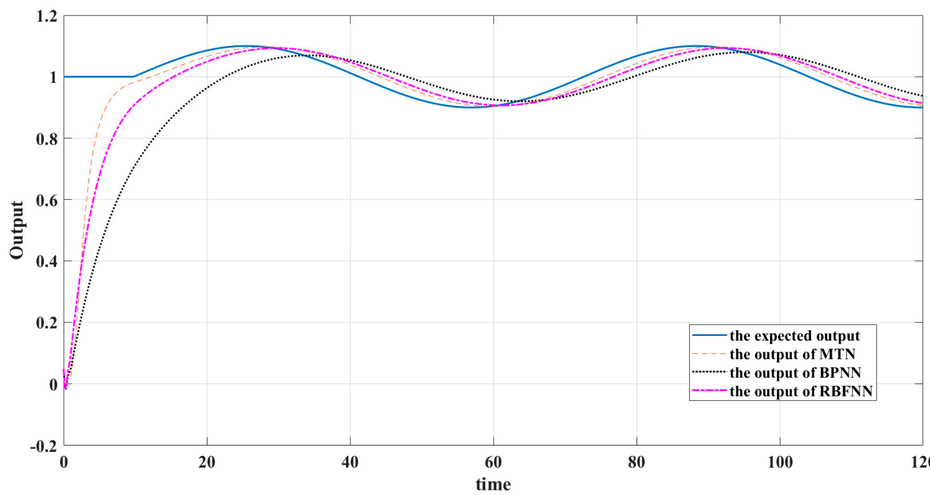

Figure 4. System output.

Similarly, the results of the three indicators are shown in Table 2.

Table 2. The tracking response comparison among three metrics obtained using different control methods.

Error Comparison	RMSE	MAE	MAPE
MTN	0.01997	0.04468	0.65589
BPNN controller	0.03958	0.10296	0.7236
RBF controller	0.02232	0.06112	0.69082

The latter figure presents the system output and the ideal tracking signal, highlighting that the system has a good tracking performance, i.e., the effectiveness of the proposed method is highlighted from the simulation results.

8. Discussion

This paper proposes an output feedback control method based on the MTN that is appropriate for non-linear strict systems so that the system output can automatically track the desired signal. The original strict-feedback system is first transformed in the proposed method, and the state variables are redefined to obtain the new standard form. A state observer is then designed to complete the identification process of the adaptive system under the good approximation characteristics of the MTN. Based on this, the adaptive control law is designed to complete the system tracking process. Numerical simulations on a servo-hydraulic system model as the control object verify the effectiveness of the suggested method.

Author Contributions: Methodology, Q.S. and Y.Z.; Software, Q.S.; Validation, S.W.; Formal analysis, X.J.; Investigation, Q.S. and C.Z.; Writing—original draft, Q.S. All authors have read and agreed to the published version of the manuscript.

Funding: This work was supported in part by the Natural Science Foundation of the Higher Education Institutions of Jiangsu Province, China (Grant No. 22KJB510026), as a subject of Educational Informatization in Colleges and Universities in Jiangsu Province (Grant No. 2021JSETKT062), as a research topic of Modern Educational Technology in Jiangsu Province (Grant No. 2022-R-101321), as part of research on Quality Assurance and Evaluation of Higher Education in Jiangsu Province (Grant No. 2021JSETKT062), as part of the Entrepreneurship Training Program for College students in Jiangsu Province (Grant No. 202210298001T), from the State Scholarship Fund under Grant 202108410235, by the Special Research and Promotion Program of Henan Province under Grant 212102210015, and as an Education and Teaching Reform Research and Practice Project of Henan Institute of Technology under Grant DQXY-2021005.

Data Availability Statement: The data presented in this study are available on request from the corresponding author. The data are not publicly available due to privacy.

Conflicts of Interest: The authors declare no conflict of interest.

References

1. Farias, A.R.; Leonardo, A.B.T.; Martinez, P.R. Distributed Control of Networked Nonlinear Systems via Interconnected Takagi-Sugeno Fuzzy Systems With Nonlinear Consequent. *IEEE Trans. Syst. Man Cybern. Syst.* **2019**, *51*, 4858–4867. [CrossRef]
2. Cao, R.W.; Su, E.C.; Lu, M.H. Comparative Study of Permanent Magnet Assisted Linear Switched Reluctance Motor and Linear Flux Switching Permanent Magnet Motor for Railway Transportation. *IEEE Trans. Appl. Supercond.* **2020**, *30*, 3601205. [CrossRef]
3. Jones, C.E.; Norman, P.J.; Sztykiel, M.; Alzola, R.P.; Burt, G.M.; Galloway, S.J.; Kawashita, L.F.; Hallett, S.R. Electrical and thermal effects of fault currents in aircraft electrical power systems with composite aero-structures. *IEEE Trans. Transport. Electrific.* **2018**, *4*, 660–670. [CrossRef]
4. Van, M.; Mavrovouniotis, M.; Ge, S.S. An adaptive backstepping nonsingular fast terminal sliding mode control for robust fault tolerant control of robot manipulators. *IEEE Trans. Syst. Man Cybern. Syst.* **2019**, *49*, 1448–1458. [CrossRef]
5. Chu, Y.; Fei, J.; Hou, S. Adaptive global sliding-mode control for dynamic systems using double hidden layer recurrent neural network structure. *IEEE Trans. Neural Netw. Learn. Syst.* **2020**, *31*, 1297–1309. [CrossRef]
6. Lu, Y. Adaptive-fuzzy control compensation design for direct adaptive fuzzy control. *IEEE Trans. Fuzzy Syst.* **2018**, *26*, 3222–3231. [CrossRef]
7. Hu, C.H.; Li, P.P.; Pan, Z. Phenotyping of poplar seedling leaves based on a 3D visualization method. *Int. J. Agric. Biol. Eng.* **2018**, *11*, 145–151. [CrossRef]
8. Bao, Y.J.; Chan, K.J.; Mesbah, A.; Velni, J.M. Learning-based adaptive-scenario-tree model predictive control with improved probabilistic safety using robust Bayesian neural networks. *Int. J. Robust Nonlinear Control* **2023**, *33*, 3312–3333. [CrossRef]
9. Bao, Y.J.; Velni, J.M. Safe control of nonlinear systems in LPV framework using model-based reinforcement learning. *Int. J. Control* **2023**, *96*, 1078–1089. [CrossRef]
10. Liu, X.; Hu, C.; Li, P. Automatic segmentation of overlapped poplar seedling leaves combining mask R-CNN and DBSCAN. *Comput. Electron. Agric.* **2020**, *178*, 105753. [CrossRef]
11. Chu, Y.; Fei, J.; Hou, S. State Ffeedback temperature control based on a smith predictor in a precalciner of a cement Kiln. *IEEE Lat. Am. Trans.* **2021**, *19*, 138–146.
12. Huang, J.T. Adaptive fuzzy state/output feedback control of nonstrict-feedback systems: A direct compensation approach. *IEEE Trans. Cybern.* **2019**, *49*, 2046–2059. [CrossRef] [PubMed]
13. Xu, J.J.; Zhang, H.S. Output feedback control for irregular LQ problem. *IEEE Control Syst. Lett.* **2021**, *5*, 875–880. [CrossRef]
14. Egidio, L.N.; Deaecto, G.S. Dynamic output feedback control of discrete-time switched affine systems. *IEEE Trans. Autom. Control* **2021**, *66*, 4417–4423. [CrossRef]
15. Yang, Y.N.; Yan, Y. Backstepping sliding mode control for uncertain strict-feedback nonlinear systems using neural-network-based adaptive gain scheduling. *J. Syst. Eng. Electron.* **2018**, *29*, 580–586.
16. Szanto, N.; Narayanan, V.; Jagannathan, S. Event-sampled direct adaptive NN output- and state-feedback control of uncertain strict-feedback system. *IEEE Trans. Neural Netw. Learn. Syst.* **2018**, *29*, 1850–1863. [CrossRef]
17. Tong, S.; Sun, K.; Sui, S. Observer-based adaptive fuzzy decentralized optimal control design for strict-feedback nonlinear large-scale systems. *IEEE Trans. Fuzzy Syst.* **2018**, *26*, 569–584. [CrossRef]
18. Li, Y.X.; Yang, G.H. Model-based adaptive event-triggered control of strict-feedback nonlinear systems. *IEEE Trans. Neural Netw. Learn. Syst.* **2018**, *29*, 1033–1045. [CrossRef]
19. Xu, B.; Shou, Y.; Luo, J.; Pu, H.; Shi, Z. Neural learning control of strict-feedback systems using disturbance observer. *IEEE Trans. Neural Netw. Learn. Syst.* **2019**, *30*, 1296–1307. [CrossRef]

20. Xu, B.; Yang, D.; Shi, Z.; Pan, Y.; Chen, B.; Sun, F. Online recorded data-based composite neural control of strict-feedback systems with application to hypersonic flight dynamics. *IEEE Trans. Neural Netw. Learn. Syst.* **2018**, *29*, 3839–3849.
21. Sun, Q.M.; Yan, H.S. Multi-dimensional Taylor Network Modelling and Optimal Control of SISO Non-linear Systems for Tracking by Output Feedback. *IMA J. Math. Control Inf.* **2019**, *37*, 699–717. [CrossRef]
22. Yan, H.S.; Duan, Z.Y. Tube-based model predictive control using multidimensional Taylor network for nonlinear time-delay systems. *IEEE Trans. Autom. Control* **2021**, *66*, 2099–2114. [CrossRef]
23. Yan, H.S.; Kang, A.M. Asymptotic tracking and dynamic regulation of SISO non-linear system based on discrete multi-dimensional Taylor network. *IET Control Theory Appl.* **2017**, *11*, 1619–1626. [CrossRef]
24. Kang, A.M.; Yan, H.S. Stability analysis and dynamic regulation of multi-dimensional Taylor network controller for SISO nonlinear systems with time-varying delay. *ISA Trans.* **2018**, *73*, 31–39. [CrossRef] [PubMed]
25. Han, Y.Q.; Zhu, S.L.; Yang, S.G. Adaptive multi-dimensional Taylor network tracking control for a class of stochastic nonlinear systems with unknown input dead-zone. *IEEE Access* **2018**, *6*, 34543–34554. [CrossRef]
26. Han, Y.Q.; Yan, H.S. Adaptive multi-dimensional Taylor network tracking control for SISO uncertain stochastic non-linear systems. *IET Control Theory Appl.* **2018**, *12*, 1107–1115. [CrossRef]
27. Levant, A. Higher-order sliding modes, differentiation and output-feedback control. *Int. J. Control* **2023**, *76*, 9–10. [CrossRef]
28. Na, J.; Dong, Y.; Ding, H.G.; Han, S.C. Output feedback control for hydraulic servo systems with unknown actuator dynamics. *Control Decis.* **2020**, *35*, 1077–1084.
29. Bao, Y.J.; Thesma, V.; Velni, J.M. Physics-guided and Neural Network Learning-based Sliding Mode Control. *IFAC Pap.* **2021**, *54*, 705–710. [CrossRef]